J. Biochem. 2009;146(6)857–866
doi:10.1093/jb/mvp146

Inhibition of Electron Acceptance from Ascorbate by the Specific *N*-carbethoxylations of Maize Cytochrome b_{561}: A Common Mechanism for the Transmembrane Electron Transfer in Cytochrome b_{561} Protein Family†

Nobuyuki Nakanishi[1], Md Motiur Rahman[1], Yoichi Sakamoto[2], Masahiro Miura[2], Fusako Takeuchi[3], Sam-Yong Park[4] and Motonari Tsubaki[2,*]

[1]Department of Molecular Science and Material Engineering, Graduate School of Science and Technology; [2]Department of Chemistry, Graduate School of Science, Kobe University, 1-1 Rokkodai-cho, Nada-ku, Kobe, Hyogo 657-8501; [3]Department of Pharmacy, College of Pharmaceutical Sciences, Ritsumeikan University, Kusatsu, Shiga 525-8577; and [4]Protein Design Laboratory, Division of Science of Biological Supramolecular Systems, Graduate School of Integrated Science, Yokohama City University, Yokohama, Kanagawa 230-0045, Japan

Received July 6, 2009; accepted August 8, 2009; published online September 16, 2009

Cytochromes b_{561} constitute a novel class of proteins in eukaryotic cells with a number of highly relevant common features including six transmembrane α-helices and two haem groups. Of particular interest is the presence of a large number of plant homologues having putative ascorbate- and monodehydroascorbate radical-binding sites. We conducted a diethylpyrocarbonate-modification study employing *Zea mays* cytochrome b_{561} heterologously expressed in *Pichia pastoris* cells. Pre-treatment of cytochrome b_{561} with diethylpyrocarbonate in oxidized form caused *N*-carbethoxylation of His^{86}, His^{159} and Lys^{83}, leading to a drastic inhibition of the electron transfer from ascorbate. The activity was protected by the inclusion of ascorbate during the treatment. However, midpoint potentials of two haem centres did show only slight decreases upon the treatment, suggesting that changes in the midpoint potentials were not the major cause of the inhibition. Present results indicated that *Zea mays* cytochrome b_{561} conducted an ascorbate-specific transmembrane electron transfer by utilizing a concerted H^+/e^- transfer mechanism and that the specific *N*-carbethoxylation of haem axial His^{86} that would inhibit the removal of a proton from the bound ascorbate was a major cause of the inhibition. On the other hand, Lys^{83} might be important for an initial step(s) of the fast electron acceptance from ascorbate.

Key words: ascorbate, cytochrome b561, transmembrane electron transfer, redox potential.

Abbreviations: DEPC, diethylpyrocarbonate; AsA, ascorbate; MDA, monodehydroascorbate; Zmb_{561}, *Zea mays* cytochrome b_{561}; WT, wild-type; MALDI-TOF, matrix assisted laser desorption/ionization-time of flight.

The cytochrome b_{561} protein family is a novel class of transmembrane proteins present in large variety of eukaryotic cells and might have a role(s) for the transmembrane electron transfer (*1*). To accomplish the electron transfer, they maintain a number of highly relevant common structural features including six hydrophobic transmembrane α-helices and two haem *b* ligation sites (*2*, *3*). Previously, we employed diethylpyrocarbonate (DEPC[7]) for the studies on the electron transfer mechanism of animal cytochromes b_{561} (*4*). DEPC is well known as a chemical modification reagent possessing high selectivity towards a de-protonated nitrogen atom of an imidazole ring of His residues and with a lesser reactivity to Lys, Tyr or other amino acid residues (*5*). We previously showed that DEPC treatment of bovine cytochrome b_{561} in oxidized form caused a significant inhibition of the electron transfer from ascorbate (AsA) and such inhibition was likely caused by the specific *N*-carbethoxylation of the haem axial His residue(s) (*4*, *6*). We proposed further that the haem axial His residue might be responsible for the 'concerted H^+/e^- transfer mechanism' at the cytosolic haem centre to withdraw a proton from the bound AsA molecule to facilitate the electron transfer to the cytosolic haem iron (*7*).

Recently, we have succeeded in the functional heterologous expression of cytochrome b_{561} from maize

†A preliminary account of present study was presented at MHS2008 (2008 International Symposium on Micro-NanoMechatronics and Human Science) (November 6–9, 2008, Nagoya, Japan).

*To whom correspondence should be addressed. Tel/Fax: +81-78-803-6582, E-mail: mtsubaki@kobe-u.ac.jp

(*Zea mays*) using yeast *Pichia pastoris* cells (*8*) (Nakanishi *et al*., unpublished data). In our preliminary study, we conducted a DEPC treatment on the purified recombinant *Zea mays* cytochrome b_{561} (WT-Zmb_{561}) and its site-directed mutants to clarify the mechanism of the inhibition on the AsA-specific electron transfer (*9*). Pre-treatment of WT-Zmb_{561} with DEPC in oxidized form caused a drastic inhibition of the electron transfer from AsA. These results suggested that plant cytochrome b_{561} also performed an AsA-related transmembrane electron transfer by utilizing a very similar molecular mechanism with those of animal cytochromes b_{561} despite of its lower conservation in amino acid sequence and, therefore, only a few amino acid residues were responsible for the electron transfer (*7*). In the present study, we extended such DEPC-modification studies to clarify the molecular mechanism responsible for the AsA-specific transmembrane electron transfer.

MATERIALS AND METHODS

Preparation of Zea Mays b_{561}/pPICZB construct, expression of recombinant Zea Mays cytochrome b_{561} and its purification—*Zea mays* cytochrome b_{561} (Zmb_{561}) cDNA (AB182641; DDBJ/EMBL/GenBank) was ligated into *EcoRI–XbaI* site of pPICZB vector to utilize the AOX1 promoter for the control of the gene expression, as described previously (*8*) (Nakanishi *et al*., unpublished data). The resulting pPICZB-WTZmb_{561} plasmid was further modified at the 3′-end of the open reading frame to have a hexa histidine (6xHis)-tag sequence in the expressed protein, and was inserted into the pPICZB vector. The resulting expression vector, pPICZB-WTZmb_{561}-H_6, could produce the recombinant *Zea mays* cytochrome b_{561} protein having a C-terminal 6xHis-tag moiety (WT-Zmb_{561}-H_6) with the amino acid sequence of ^{211}GASVVVAAIAPVRLEEPQGYDPIPENHHHHHH^{242} in its C-terminal region. These two expression vectors were each linearized with *Pme*I and were transformed into *Pichia pastoris* GS115 competent cells (His^-, Mut^+) (Invitrogen, Carlsbad, CA, USA) to give a methanol-inducible WT-Zmb_{561} expression. The transformants were selected on YPDS plates containing zeocin (100 μg/ml). Following procedures including, culture, protein induction, preparation of microsomal fractions, and purification of WT-Zmb_{561} or WT-Zmb_{561}-H_6, were conducted according to the methods previously described (*8*).

DEPC treatment of Zea Mays cytochrome b_{561}—The oxidized WT-Zmb_{561} solution was diluted to 10 μM with 50 mM potassium phosphate buffer (pH 7.0) containing 1.0% (w/v) *n*-octyl-β-glucoside. The sample was treated with 0.5 mM DEPC for 30 min, as previously described (*4*, *6*). During the DEPC treatment, difference spectra in UV-visible region were recorded with a Shimadzu UV-2400PC spectrophotometer (Kyoto, Japan). The DEPC-treated samples were, then, gel-filtered through a PD-10 column equilibrated with 50 mM potassium phosphate buffer (pH 7.0) containing 1.0% (w/v) *n*-octyl-β-glucoside to remove unreacted DEPC.

Stopped-flow analysis—Rapid kinetic measurements were carried out using an RSP-100-03DR stopped-flow rapid-scan spectrometer (UNISOKU Co. Ltd, Osaka, Japan), as previously described (*10*). One chamber of the apparatus contained oxidized form of WT-Zmb_{561} or its DEPC-treated derivative (2.0 μM or indicated in the text) in 50 mM potassium phosphate (pH 7.0) buffer containing 1.0% *n*-octyl-β-glucoside. The other chamber contained a test concentration of AsA (2, 4, 8 and 16 mM) in the same buffer. The temperature of both chambers and the sample holder was maintained at 20°C by connecting to a thermobath (Tokyo Rikakikai Co. Ltd, Model NCB-1200; Tokyo, Japan). The mixing was carried out with a 1 : 1 (v/v) ratio. Haem reduction of WT-Zmb_{561} (or its DEPC-treated derivative) was followed spectrophotometrically by absorbance change at 427 nm using a photomultiplier and data points were collected in every 2.5 ms during the 10 s measurements (total 4,000 data points). The time-courses of the absorbance change were fitted by use of a non-linear least-squares method of a built-in software of the apparatus or IgorPro (v. 6.0) software with a single (or a linear combination of) exponential decay equations.

Redox titrations—Spectroscopic titrations were performed essentially as described by Dutton (*11*) and Takeuchi (6), using a Shimadzu UV-2400PC spectrometer equipped with a thermostatted cell holder connected to a low temperature thermobath (NCB-1200, Tokyo Rikakikai Co Ltd, Tokyo, Japan). A custom anaerobic cuvette (1 cm light path, 5 ml sample volume) equipped with a combined platinum and Ag/AgCl electrode (6860-10C, Horiba, Tokyo, Japan) and a screw-capped side arm was used. Purified WT-Zmb_{561} sample or its DEPC-treated sample (final, 10 μM) in 50 mM potassium phosphate buffer (pH 7.0) containing 1.0% (w/v) octyl β-glucoside was mixed with redox mediators (potassium ferricyanide, 60 μM; quinhydrone, 20 μM; 1,2-naphthoquinone, 20 μM; phenazine methosulphate, 20 μM; duroquinone, 40 μM; 2-hydroxy-1,4-naphtoquinone, 5 μM; riboflavin, 20 μM). The sample solution was kept under a flow of moistened argon gas to exclude dioxygen and was continuously stirred with a small magnetic stirrer (CC-301, SCINICS, Tokyo, Japan) inside. Reductive titration was performed at 15°C by addition of small aliquots of sodium dithionite solution (5 or 20 mM) through a needle in the rubber septum on the side arm; for a subsequent oxidative titration, potassium ferricyanide (5 or 20 mM) was used as the titrant. In an appropriate interval, visible absorption spectra and redox potentials were recorded. The changes in absorbance ($A_{561.0}$ minus $A_{566.8}$, the isosbestic point of WT-Zmb_{561}) were corrected with the dilution effect and analyzed with Igor Pro (v. 6.0) employing a Nernst equation with two redox components.

RESULTS

Inhibition of the electron acceptance from AsA by modification with DEPC—DEPC is well known as a chemical modification reagent possessing high selectivity towards an imidazole ring of His residues (*5*) and with a lesser extent to Lys residues. DEPC-treatment of the purified WT-Zmb_{561} in oxidized form was conducted at two different molar ratios (DEPC: WT-Zmb_{561} = 50 : 1

and 16 : 1). As the reaction proceeded, slight absorbance changes in both UV and Soret regions were observed (Fig. 1A). The changes in the UV region indicated that chemical modifications occurred on some His residues (Fig. 1A, inset) exposed to solvents and/or the haem-coordinating His residues. Extent of *N*-carbethoxylation of His residues was calculated based on the absorbance change at 240 nm (ΔA_{240}) using a molar extinction coefficient of 3.2 $mM^{-1}cm^{-1}$ for *N*-carbethoxylated histidine (*5*). The number of *N*-carbethoxylated His residue was estimated as 1.9 for both of the samples being DEPC-treated with molar ratios of 50 : 1 and 16 : 1. Considering the total number of His residues (*8*) in the deduced amino acid sequence of WT-Zmb_{561}, this value was much fewer than the corresponding values observed for cytochrome b_5 (*12*) and for six coordinated porcine

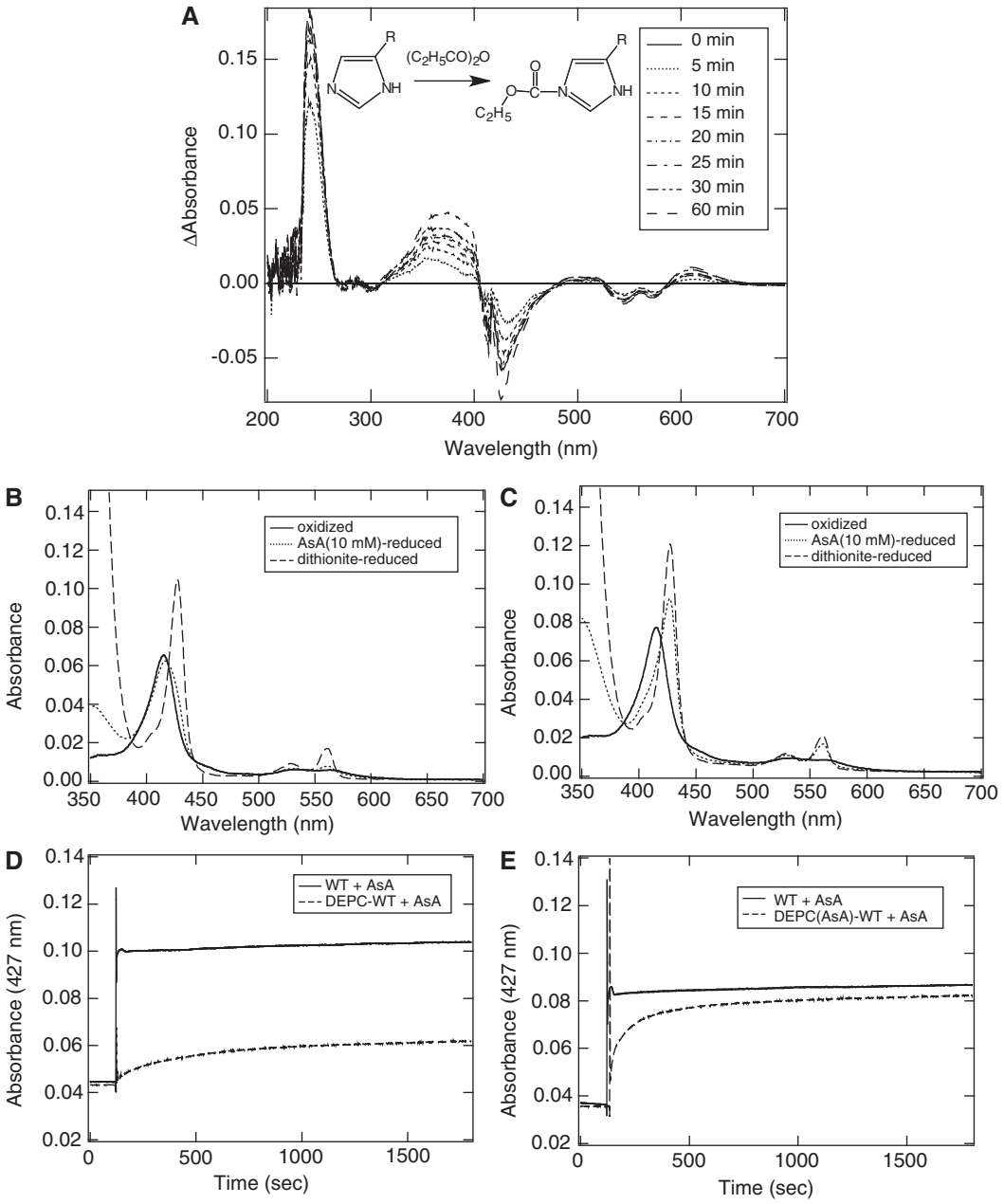

Fig. 1. **Effects of DEPC treatment on the UV-visible absorption spectra of purified recombinant *Zea mays* cytochrome b_{561} (WT-Zmb_{561}).** (A) Difference spectral change after the addition of DEPC to the oxidized form of WT-Zmb_{561}. As the reaction proceeded, increase in absorbance at 240 nm due to the formation of *N*-carbethoxyl histidine residues was observed. (B and C) Absorption spectra of WT-Zmb_{561} pre-treated with DEPC in the absence (B) or presence (C) of AsA (10 mM). Solid line, oxidized form; dotted line, AsA(10 mM)-reduced form; broken line, dithionite-reduced form. (D and E) Time courses of A_{425} of WT-Zmb_{561} pre-treated with DEPC in the absence (D) or presence (E) of AsA (10 mM) after mixing with AsA (10 mM) (broken line in each panel). In each panel, control (untreated WT-Zmb_{561}) experiment was shown in a solid line.

myoglobin mutant (VHA-Mb) (*13*) upon the DEPC treatments under similar experimental conditions. The concerted progress in absorbance changes at Soret and UV regions (Fig. 1A) indicated that the *N*-carbethoxylation of His residues occurred at or near the haem centre(s).

Interestingly, we found that the DEPC treatment of WT-Zmb_{561} caused a significant inhibition of its electron acceptance ability from AsA. As shown in Fig. 1B, visible absorption spectrum of the DEPC pre-treated WT-Zmb_{561} after the addition of AsA (10 mM) showed no clear development of sharp peaks around α and β region in the visible absorption spectrum; however, in the dithionite-reduced form, there were clear peaks at 561, 530 and 427 nm, indicating the full-reduction of two haem centres without any structural damage around the haem centre upon the DEPC treatment. The final reduction level of two haem centres in the DEPC-treated WT-Zmb_{561} with AsA (10 mM) as a reductant was <40%. This specific inhibition of the electron acceptance from AsA caused by the DEPC modification had a very similar precedence for bovine cytochrome b_{561}, in which the final reduction level with AsA was ~30% (*4*, *6*). On the other hand, oxidized WT-Zmb_{561} pre-treated with DEPC in the presence of 10 mM AsA was easily reduced with AsA (10 mM) with the final reduction level of 76%, which was almost the same level with that of untreated WT-Zmb_{561}. These results suggested that, in the presence of AsA, a relatively stable AsA - WT-Zmb_{561} binary complex might be formed and such a formation of the complex would protect a key amino acid residue(s) from the attack of DEPC reagent, resulting in the prevention against a loss of the electron accepting ability from AsA. However, when the time courses of the two reduction processes at 427 nm were examined carefully, there was still a significant difference in the reaction rate between two kinds of the DEPC-treated samples (Fig. 1D and E). Thus, inclusion of AsA during the DEPC treatment caused a clear protective effect on the final haem reduction level with AsA as a reductant, but it was not sufficient to protect the fast reduction rate. To confirm this point further, we conducted stopped-flow analyses on the DEPC-treated WT-Zmb_{561} for the reaction with AsA (Fig. 2). With a concentration of AsA as 8.0 mM (final) at pH 7.0, oxidized WT-Zmb_{561} was reduced quickly with $k_{app} = 8.6\,s^{-1}$ for the fastest phase (Fig. 2; line a). The DEPC treatment in the oxidized form caused a drastic loss of the fast reduction process and k_{app} was estimated as $0.06\,s^{-1}$ (Fig. 2; line c), which was less than 1/100 of the fastest phase of the untreated WT-Zmb_{561}. Inclusion of AsA (10 mM) during the DEPC treatment protected the electron accepting ability from AsA but k_{app} was still $0.139\,s^{-1}$ (Fig. 2; line b), about 1/50 of the fastest phase of the untreated sample.

Identification of the DEPC-modified residues by MALDI-TOF peptide mapping analyses—To clarify the key amino acid residue(s) responsible for the electron acceptance from AsA, we searched DEPC-modification sites by utilizing MALDI-TOF mass spectrometry. UV-visible difference spectral change upon the DEPC treatment indicated that the number of *N*-carbethoxylated histidyl residues was 1.9 per

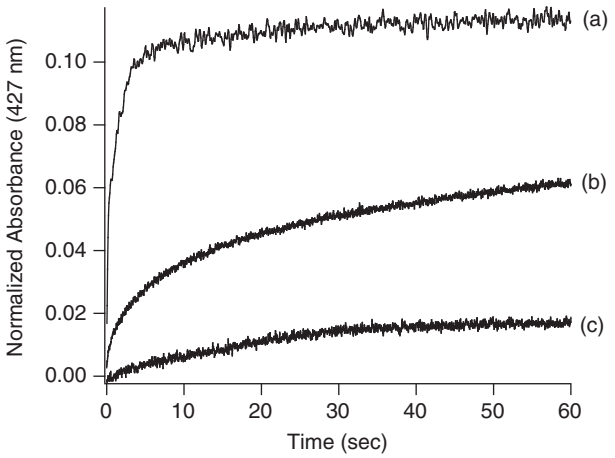

Fig. 2. **Inhibition of the electron acceptance from AsA by the DEPC treatment for the purified recombinant *Zea mays* cytochrome b_{561} (WT-Zmb_{561}) as analysed by stopped-flow spectrometry.** The electron accepting reaction from AsA (final 8 mM) of 1 μM (final) oxidized WT-Zmb_{561} (line a) or WT-Zmb_{561} pre-treated with DEPC in the presence (line b) or absence (line c) of AsA (10 mM) in 50 mM potassium phosphate buffer (pH 7.0) containing 1.0% *n*-octyl-β-glucoside was measured by stopped-flow spectrometry using two solution mixing system with a 1:1 volume ratio. Increases in absorbance at 425 nm due to the reduction of the haem centres were recorded. Other conditions are described in the text.

WT-Zmb_{561} molecule. Careful analyses of the MALDI-TOF mass spectra of the protease-digested WT-Zmb_{561} (with either TPCK-treated trypsin or V8 protease) for the sample treated with DEPC (50:1, 16:1 molar ratio) indicated that several amino acid residues were modified with DEPC, as evidenced by the appearance of several peptides showing a mass increment of 72 (m/z) (*4*, *6*). Comparison of the mass spectra of the proteolytic digests in considering the nucleophilicity of amino acid residues, possible modification sites in the tryptic peptides (Fig. 3A and B, Table 1) could be listed as follows. (i) No major modification site for peptides 1–8, 36–45, 46–72, 107–152 and 224–236. (ii) One major and one minor sites in peptide 9–35 (possible sites; Tyr^{14} and His^{17}). (iii) Two major and one minor sites in peptide 73–106 (possible sites; His^{79}, Lys^{83}, His^{86}, His^{90} and Tyr^{102}). (iv) One major and two minor sites in peptide 154–192 (possible sites; His^{159}, Tyr^{167} and Lys^{182}). (v) One minor site in peptide 193–223 (possible site; Tyr^{193}). Similarly, possible modification sites in the V8 protease peptides (Fig. 3C and Table II) could be listed as follows. (vi) No major modification sites for peptides 42–66, 67–80, 176–186, 197–236. (vii) One major and one minor sites in peptide 1–41 (possible sites; Tyr^{14} and His^{17}). (viii) Two major and two minor sites in peptide 81–110 (possible sites; Lys^{83}, His^{86}, His^{90} and Tyr^{102}). (xi) One major and one minor sites in peptide 111–175 (possible sites; His^{159} and Tyr^{167}). (x) One minor site in peptide 187–196 (possible site; Lys^{192}). Prolonged incubation with TPCK-treated trypsin or V8 protease at room temperature resulted in cleavages other than the authentic cleavage sites, leading to a formation of shorter polypeptides (results not shown). From the analysis of these

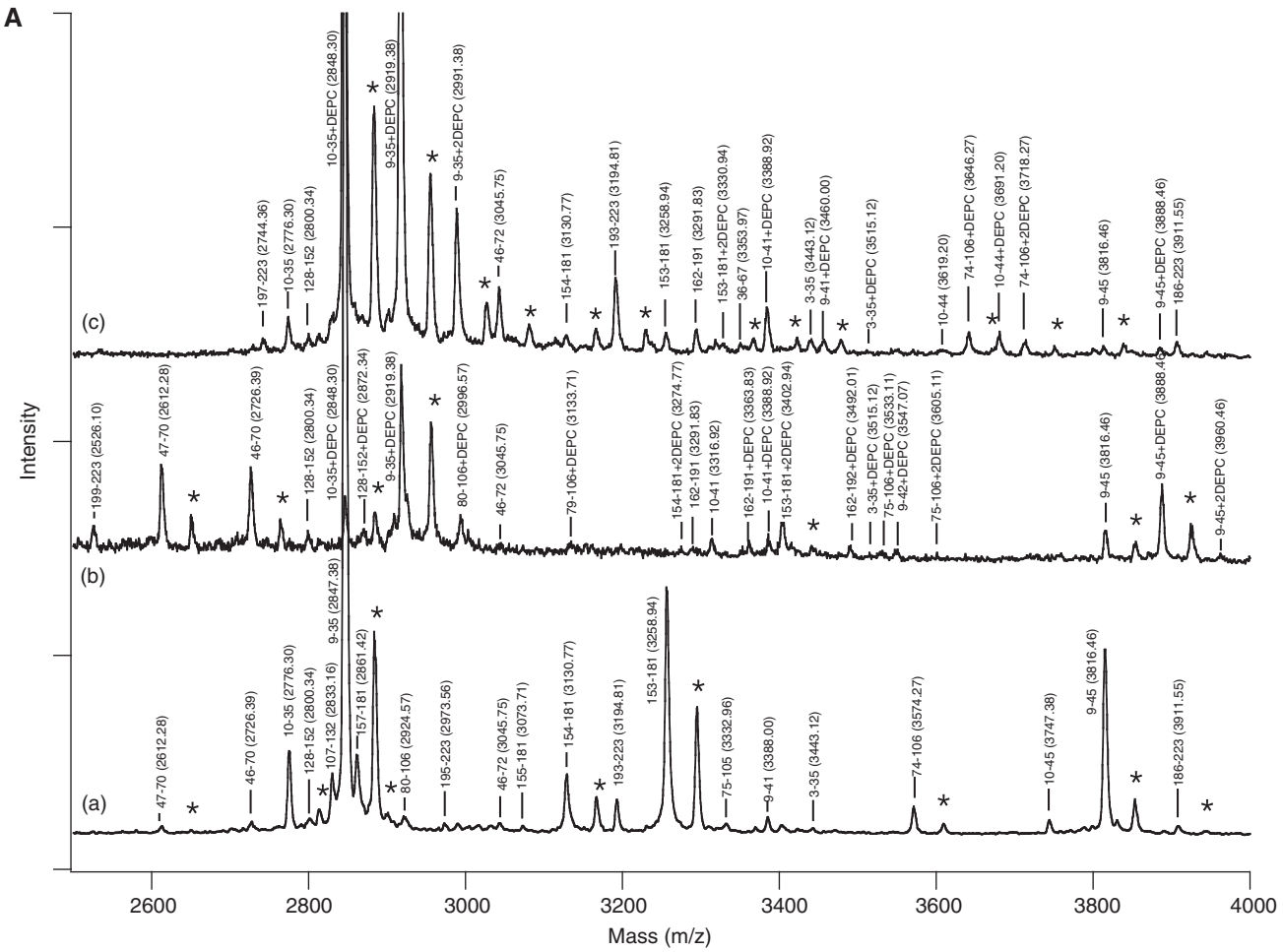

Fig. 3. **MALDI-TOF mass spectra of the protease-digested fragments from purified recombinant WT-Zmb_{561} with or without the DEPC treatment.** The DEPC-treated (in the presence or absence of 10 mM AsA) and untreated recombinant WT-Zmb_{561} samples in 50 mM potassium phosphate (pH 7.0) buffer containing 1.0% *n*-octyl-β-glucoside were each treated with TPCK-trypsin (A and B) or V8 protease (C) and the digested sample solutions were directly mixed with the matrix solution [1 : 9 (v/v)] as described in the text. MADLI-TOF mass spectrometry was carried out with a Voyager DE Pro mass spectrometer (Applied Biosystem) using a 20-kV accelerating voltage. In each panel, line (a) indicates the untreated sample, line (b) indicates the sample pre-treated with DEPC in the absence of AsA, and line (c) indicates the sample pre-treated with DEPC in the presence of AsA (10 mM). Asterisks indicated the $[M+K^+]$ form. Other conditions are described in the text.

polypeptides, we conclude that there are three major DEPC-modification sites at Lys^{83}, His^{86} and His^{159} for oxidized WT-Zmb_{561}.

The Lys^{83} residue locating on the cytosolic side of the molecule is a highly conserved residue in all the members of cytochrome b_{561} family (2). On the other hand, His^{86} and His^{159} are axial ligands of the cytosolic haem centre (*1*). Although exact evaluation of the extent of the modification was difficult based on the MALDI-TOF mass spectra, we noticed that the extent of *N*-carbethoxylation at Lys^{83} was not so significant as that of Lys^{85} residue in bovine cytochrome b_{561} (*4*, *6*).

Involvement of the three conserved residues (Lys^{83}, His^{86} and His^{159}) for the electron acceptance from AsA was further analysed by the protecting effect of AsA against the loss of the electron transfer activity caused by the DEPC treatment. When the tryptic peptides of DEPC-treated WT-Zmb_{561} in the presence or absence of AsA (10 mM) were compared with MALDI-TOF mass spectrometry, we found that modification level of His^{86} was suppressed significantly by the inclusion of AsA during the DEPC modification (Fig. 3A–C). For other two amino acid residues, we could not observe any significant protective effect.

Additional moderate or weaker modifications with DEPC were found at His^{17}, His^{79} and Lys^{192}, with the His^{17} residue as the most prominent one (Fig. 3A, Tables 1 and 2). We considered that these additional modifications did not have significant roles in the inhibition of the electron transfer activity based on the absence of the protective effect of AsA and that, therefore, these residues would not have important functional roles for the electron transfer from AsA.

We also conducted a similar treatment with DEPC for WT-Zmb_{561}-H_6. We found that the numbers of *N*-carbethoxylated histidine was 2.54 residues per

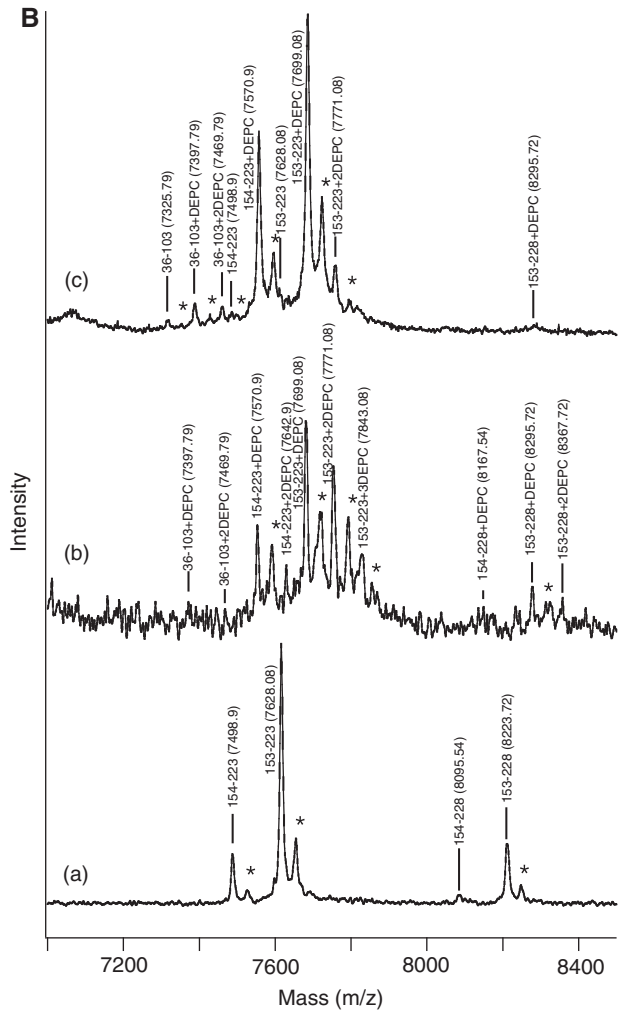

Fig. 3. Continued.

molecule and major modification sites were His^{86}, His^{159} and Lys^{83} (and non-conservative His^{17} with a slightly lower extent). Considering the total number of His residues in the amino acid sequence of WT-Zmb_{561} (eight residues) and in the additional C-terminal His-tag moiety (six residues), this small value again indicated a site-specific *N*-carbethoxylation being occurred only around the cytosolic haem centre. Similar analyses conducted on some site-specific mutants including K83A and R72D mutants (*9*) were also consistent with the present conclusion (results not shown).

Effects of DEPC modification on the redox potentials of two haem centres—We found that the DEPC treatment of WT-Zmb_{561} in oxidized form did not cause any appreciable influences on the redox potentials of two haem centres. Before the treatment, midpoint potentials of the two haem centres were estimated as +123 and +15 mV (Fig. 4A), slightly lower than those of bovine cytochrome b_{561} (+170 and +60 mV) (6). After the treatment, midpoint potentials were estimated as +104 and −8 mV (Fig. 4B), respectively, lowered by only 20–25 mV for both haem centres.

DISCUSSION

DEPC treatment caused significant inhibition in the electron transfer from AsA—The electron accepting ability of Zmb_{561} from AsA was inhibited drastically by the DEPC treatment in oxidized form [Fig. 1B and D; Fig. 2 (b)], but was protected by the inclusion of AsA (10 mM) during the treatment [Fig. 1C, E; Fig. 2(c)]. Based on the comparison of the mass spectra of protease-digested peptides for the DEPC-treated and intact WT-Zmb_{561}, major DEPC modification sites were identified as Lys^{83}, His^{86} and His^{159} (Fig. 3). Among them, the latter two are axial ligands of the cytosolic haem centre (*1*) and Lys^{83} on the cytosolic loop is highly conserved among the plant and animal cytochrome b_{561} species (2). In our previous studies using bovine cytochrome b_{561}, we observed that corresponding three residues (Lys^{85}, His^{88} and His^{161}) were major modification sites upon the DEPC treatment and proposed that the inhibition of the electron transfer from AsA was caused by the *N*-carbethoxylation of these residues (*4*, *6*). However, there was a possibility that the specificity of DEPC to these residues in bovine cytochrome b_{561} might occur by chance. Present study proved that the selective modification with DEPC of these residues in WT-Zmb_{561}, which has only 38% identity in amino acid sequences with that of bovine cytochrome b_{561}, was due to common properties of cytochrome b_{561} protein family. Being consistent with this view, DEPC treatment of partially purified cytochrome b_{561} from ethiolated bean (*Phaeseolus vulgaris* L.) hypocotyls showed a reduction level of only ~20% of dithionite reduction upon addition of AsA, and the reduction rate was much slower (*14*), although no detailed assignments were made for the modification sites.

Inhibition mechanism caused by N-carbethoxylation of axial his residues—We further proposed previously that *N*-carbethoxylation of the haem axial His residues were major cause of the inhibition in the electron acceptance from AsA for bovine cytochrome b_{561} (*4*, *6*). The most remarkable point on the DEPC reactivity to Zmb_{561} would be a fact that the haem group was not released from the protein moiety at all, as observed for bovine cytochrome b_{561} (*4*, *6*). This was not observed for human cytochrome b_5 (*12*) or a six-coordinated porcine myoglobin mutant (VHA-Mb) (*13*), in which the DEPC treatment led to either a release of the haem group or a formation of the five-coordinated high-spin haem species (*12*, *13*). DEPC is well known to react with a deprotonated nitrogen atom of the imidazole ring (*5*). Therefore, in the oxidized form of WT-Zmb_{561} (and bovine cytochrome b_{561} as well), the *N*-carbethoxylation occurred not on the haem-coordinating N_ε atom but on the deprotonated N_δ atom of the same imidazole ring. Existence of the deprotonated $N_{\delta1}$ atom only at the axial imidazole ring (a very unusual state for the axial His residues) of the cytosolic haem centre could explain the preferable modification with a relatively low concentration of DEPC. Since the concomitant proton transfer from AsA is a prerequisite step for the fast biological electron transfer from AsA to an electron donor (*15*, *16*), we speculated that a cycle of deprotonated and protonated forms of axial imidazole $N_{\delta1}$ atom at the

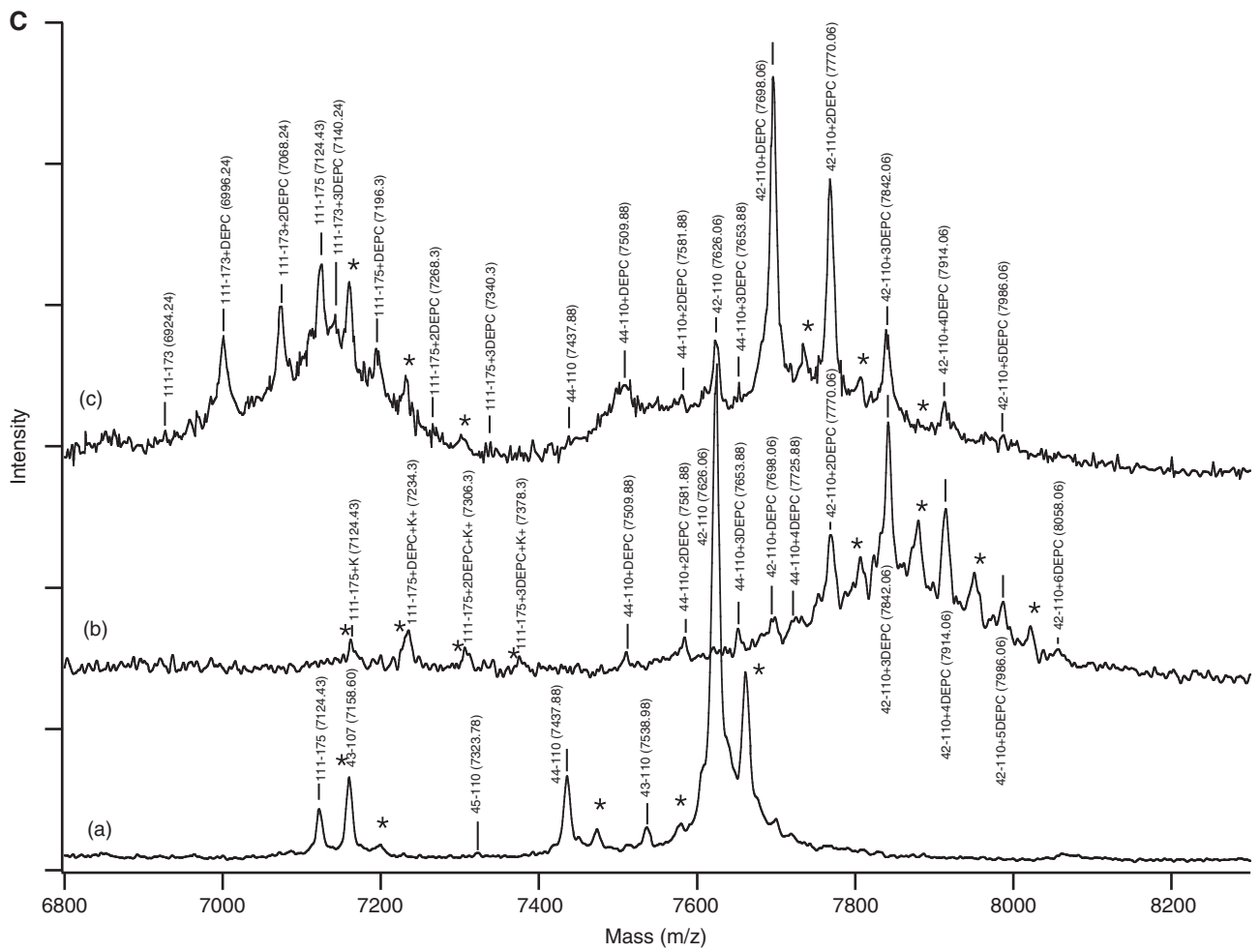

Fig. 3. Continued.

Table 1. **Theoretical tryptic fragments of the recombinant WT-Zmb_{561}.**

No.	From-To	MH^+	Sequence
1	1–8	803.02	MGLGLGVR
2	9–35	2848.39	AAPFTYAA**H**ALAVAAAAM VLVWSIQFR
3	36–45	990.10	GGLAIESTNK
4	46–72	3046.76	NLIFNVHPVLMLIGYVIIG GEAIMVYR
5	73–83	1213.33	VLPTSN**H**DTT**K**
6	84–106	2480.10	LI**H**LILHGIALVLGAVGIYFAFK
7	107–152	5066.82	NHNESGIANLYSLHSWIGIGTITL YGIQWIIGFVTFFFPGAAPNVK
8	153–153	147.20	K
9	154–181	3131.77	GVLPW**H**VLFGLFVYILALA NAELGFLEK
10	182–192	1210.37	LTFLESSGLDK
11	193–223	3195.81	YGTEAFLVNFTALVVVLFGASV VVAAIAPVR
12	224–236	1501.59	LEEPQGYDPIPEN

Theoretical tryptic peptides based on the deduced amino acid sequence of the recombinant WT-Zmb_{561} are indicated. Possible DEPC-modification sites are indicated in boldface and three major sites among them are underlined.

Table 2. **Theoretical V8 protease fragments of the recombinant WT-Zmb_{561}.**

No.	From-To	MH^+	Sequence
1	1–41	4173.00	MGLGLGVRAAPFTYAA**H**ALA VAAAAMVLVWSIQFRGGLAIE
2	42– 66	2743.29	STNKNLIFNVHPVLMLIGYVIIGGE
3	67–80	1616.88	AIMVYRVLPTSN**H**D
4	81–110	3304.95	TT**K**LI**H**LILHGIALVLGAVGIYF AFKNHNE
5	111–175	7125.44	SGIANLYSLHSWIGIGTITLYGIQW IIGFVTFFFPGAAPNVKKGV LPW**H**VLFGLFVYILALANAE
6	176–180	578.69	LGFLE
7	181–186	750.91	KLTFLE
8	187–191	478.48	SSGLD
9	192–196	597.65	KYGTE
10	197–235	4113.83	AFLVNFTALVVVLFGASVVVAAI APVRLEEPQGYDPIPE
11	236–236	133.13	N

Theoretical V8 protease-digested peptides based on the deduced amino acid sequence of the recombinant WT-Zmb_{561} are indicated. Possible DEPC-modification sites are indicated in boldface and three major sites among them are underlined.

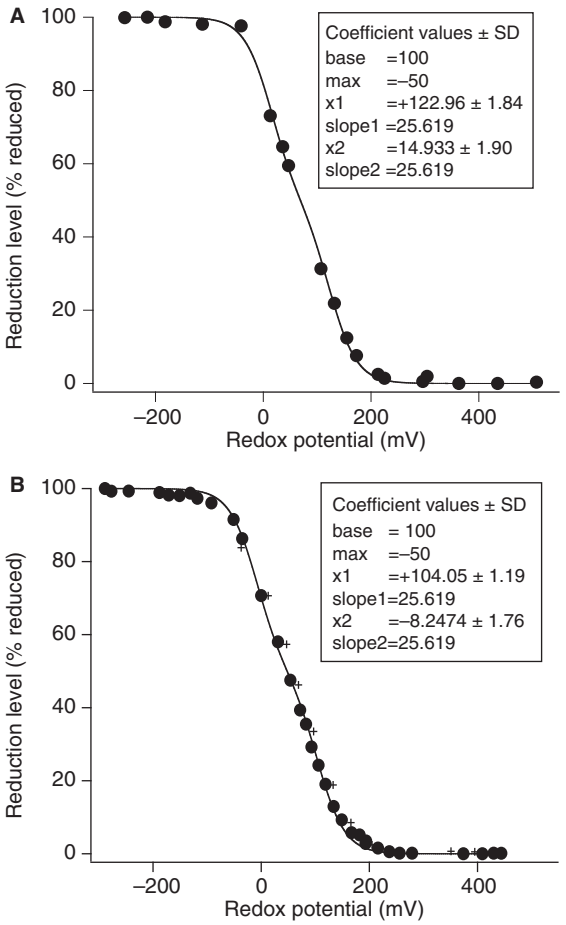

Fig. 4. **Potentiometric behavior of purified recombinant WT-Zmb_{561} (A) and effects of the DEPC treatment (B).** (A) Percentages of the reduction level were calculated based on the absorbance difference of α-band peak (561.0 nm) and an isosbetic point (566.8 nm) based on the absorption spectra of WT-Zmb_{561} poised in various redox potentials and were plotted against potentials [expressed relative to the normal hydrogen electrode (NHE)]. (B) Percentages of the reduction level of the DEPC-treated WT-Zmb_{561} were plotted against potentials as in panel A. In each panel, solid circles and crosses indicate data points for the reductive and the oxidative titrations, respectively. Least-square curve-fittings on the data points of the reductive phase were conducted by IgorPro software (v.6.0) assuming two distinct redox components [*i.e.* with a linear combination of two sigmoid functions; $f(x) = \text{base} + (\text{max}*1/(1+\exp((x_1-x)/\text{slope1}))) + (\text{max}*1/(1+\exp((x_2-x)/\text{slope2})))$, in which base, max, slope1 and slope2 were fixed as 100, −50, 25.62 and 25.62, respectively, during the curve-fitting procedure, and x_1 and x_2 gave the estimated midpoint potentials (in mV), respectively.] Other details are described in the text.

cytosolic haem centre might be essential for the fast electron acceptance from AsA in cytochrome b_{561}, as an initial step of the transmembrane electron transfer (*6*, *17*). Such specific roles of the deprotonated $N_{\delta1}$ atom in the axial imidazole group as the site to accept a proton from a bound AsA molecule for facilitating the electron acceptance from AsA ('the concerted proton/electron transfer mechanism') (Fig. 5) was discussed previously (*7*) based on the characteristic pH-dependency in the electron

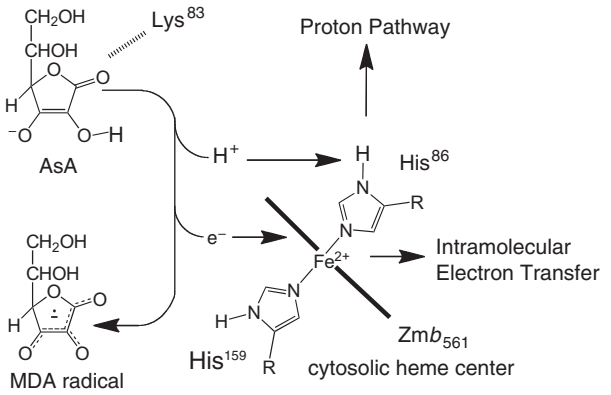

Fig. 5. **Postulated mechanism for the concerted proton/electron transfer reaction from AsA to the cytosolic haem *b* center of Zmb_{561}.** Details are described in the text.

acceptance from AsA (*17*) and the specific inhibition of the electron acceptance by the $N_{\delta1}$-carbethoxylation (*4*, *6*). Indeed, the characteristic pH-dependency in the electron acceptance from AsA was observed in a similar or even in a stronger extent for WT-Zmb_{561} in our recent study (Nakanishi *et al.*, unpublished data).

Since the haem *b* group on the cytosolic side might be lying in parallel to the membrane normal (*18*), only one of the two haem axial His residues (His^{86} and His^{159}) might actually have a role for accepting a proton from the bound AsA molecule. Although both His residues were modified with DEPC in a significant extent and were protected from the modification by the inclusion of AsA, as for bovine cytochrome b_{561} (*4*, *6*), we considered that His^{86} would have such a role (Fig. 5), as discussed previously (*7*). Being consistent with this postulation, we observed a stronger protective effect of AsA against the DEPC modification to His^{86} than to His^{159} (Fig. 3).

Interestingly, feasibility of the deprotonated His ligand(s) in the oxidation of AsA by cytochrome b_{561} by 'proton-coupled electron transfer mechanism' (*19*) has been examined experimentally using (TPP)Fe^{3+}-imidazolate complexes and an AsA-derivative (*20*). They found that deprotonation of the imidazole ligand caused a faster (more than a factor of 10) electron transfer reaction and concluded that the electron transfer occurred most likely by 'hydrogen atom transfer' (*20*). 'Hydrogen atom transfer' is a type of 'proton-coupled electron transfer reaction' in which a proton and an electron were transferred in a single kinetic step from one donor to one acceptor (*19*).

Stabilization of such an unusual de-protonated form for the axial imidazole group might be accomplished by positively charged residues on the cytosolic side, which are also responsible for the formation of the AsA-binding site near the cytosolic haem centre. Among such positively charged residues, Lys^{83} would be the most responsible one if one considered its high conservation, its spatial closeness to the cytosolic haem center, and the results of the mutation analysis on this residue (Nakanishi *et al.*, unpublished results) (*7*).

Inhibition mechanism caused by the N-carbethoxylation of Lys^{83}—We would like to propose

that Lys^{83} is responsible for the initial recognition and binding of AsA to the putative AsA-binding site. Being consistent with this view, our recent stopped-flow studies on site-specific mutants at the Lys^{83} residue (including K83A, K83D and K83E) showed significant retardation in the electron acceptance from AsA compared to that of WT-Zmb_{561} (Nakanishi *et al*., unpublished results). However, these mutations did not affect significantly on the final reduction level of the haem centres with AsA as a reductant. Interestingly, kinetic properties of these K83 mutants in the electron transfer from AsA at a neutral pH were similar to those of bovine cytochrome b_{561} pre-treated with DEPC in the presence of AsA, in which only Lys^{85} residue was *N*-carbethoxylated (6) and WT-Zmb_{561} pre-treated with DEPC in the presence of AsA [Fig. 2(b)]. These results could be explained as a loss of the electrostatic interaction between the positively charged ε-amino group and the negatively charged AsA molecule, leading to the slowed binding of AsA and the slowed electron transfer.

Careful examination showed that extent of the inhibition in the electron transfer from AsA to oxidized haem centre upon the DEPC treatment was slightly less than those previously observed for the DEPC-treated bovine cytochrome b_{561} (*4*, *17*). The slightly lower sensitivity might be ascribed partly to the lower reactivity of Lys^{83} residue to DEPC in WT-Zmb_{561} than the corresponding Lys^{85} residue in bovine cytochrome b_{561}. Alternatively, the mechanistic role of Lys^{83} residue in the interaction with the AsA molecule might be slightly lower in WT-Zmb_{561} than the corresponding one in bovine cytochrome b_{561}. It is very likely that the lower reactivity of Lys^{83} residue to DEPC might be related to a lower degree of the conservation of the putative AsA-binding motif in plant cytochrome b_{561} species (*1*).

As discussed in a previous section, Lys^{83} residue might have an additional role(s) for stabilizing the deprotonated form of the axial His residue. Further, it may be also responsible for the facilitated transfer of a proton from the axial His residue to outside of the protein matrix to prepare a next cycle of the electron acceptance from AsA. However, such arguments might be too speculative at this stage and are apparently beyond the scope of our present study. However, it must be noted that the 'the concerted proton/electron transfer mechanism' is maintained by only a limited numbers of conserved residues on the cytosolic side, which include two haem axial His residues (His^{86} and His^{159}), Lys^{83}, Arg^{72} and Tyr^{71} and these residues are also responsible for the specific DEPC reactivity.

Effects of the DEPC treatment on the redox potentials—In our previous study on bovine cytochrome b_{561}, we postulated that the decrease in the midpoint potential (90 mV decrease) of the cytosolic haem centre by the DEPC treatment was partly responsible for the inhibition of the electron acceptance from AsA (6). However, in the present study, we found that the decrease in the midpoint point potential of the cytosolic haem centre after the DEPC treatment was very slight ($\sim$20 mV) (Fig. 4), despite the final reduction levels with AsA were no much different each other. Therefore, the decrease in the midpoint potential of the cytosolic haem centre might be participating only a marginal role in the inhibition mechanism upon the DEPC treatment or it might be merely reflecting a side effect caused by the *N*-carbethoxylation of the axial His residue, at least in the case of WT-Zmb_{561}.

In conclusion, our present results indicated that the 'concerted H^+/e^- transfer mechanism' is likely to be common among the members of cytochrome b_{561} protein family. Based on the considerations for the possible inhibition mechanism of the electron transfer from AsA by the DEPC modification, we propose that Lys^{83} is important for an initial step(s) of the fast electron acceptance from AsA, whereas His^{86} is important for a later step(s) of the electron transfer and for controlling the final reduction level of the haem prosthetic group, although their roles might be not so clearly separated and would be very complex in reality. It was further postulated that the specific $N_{\delta 1}$-carbethoxylation of the haem axial His^{86} residue that would prevent the removal of a proton from the bound AsA at the cytosolic binding site was the major cause of the inhibition of the AsA-specific electron transfer upon the DEPC treatment of WT-Zmb_{561}.

FUNDING

Grants-in-Aid for Scientific Research on Priority Areas (System Cell Engineering by Multi-scale Manipulation; 18048030 and 20034034 to M. T.) from the Japanese Ministry of Education, Science, Sports and Culture.

CONFLICT OF INTEREST

None declared.

REFERENCES

1. Tsubaki, M., Takeuchi, F., and Nakanishi, N. (2005) Cytochrome b561 protein family: expanding roles and versatile transmembrane electron transfer abilities as predicted by a new classification system and protein sequence motif analyses. *Biochim. Biophys. Acta* **1753**, 174–190
2. Okuyama, E., Yamamoto, R., Ichikawa, Y., and Tsubaki, M. (1998) Structural basis for the electron transfer across the chromaffin vesicle membranes catalyzed by cytochrome b_{561}: analyses of cDNA nucleotide sequences and visible absorption spectra. *Biochim. Biophys. Acta* **1383**, 269–278
3. Tsubaki, M., Nakayama, M., Okuyama, E., Ichikawa, Y., and Hori, H. (1997) Existence of two heme B centers in cytochrome b_{561} from bovine adrenal chromaffin vesicles as revealed by a new purification procedure and EPR spectroscopy. *J. Biol. Chem.* **272**, 23206–23210
4. Tsubaki, M., Kobayashi, K., Ichise, T., Takeuchi, F., and Tagawa, S. (2000) Diethylpyrocarbonate-modification abolishes fast electron accepting ability of cytochrome b_{561} from ascorbate but does not influence on electron donation to monodehydroascorbate radical: distinct roles of two heme centers for electron transfer across the chromaffin vesicle membranes. *Biochemistry* **39**, 3276–3284
5. Miles, E. W. (1977) Modification of histidyl residues in proteins by diethylpyrocarbonate. *Methods Enzymol.* **47**, 431–442
6. Takeuchi, F., Kobayashi, K., Tagawa, S., and Tsubaki, M. (2001) Ascorbate inhibits the carbethoxylation of two histidyl and one tyrosyl residues indispensable for the transmembrane electron transfer reaction of cytochrome b_{561}. *Biochemistry* **40**, 4067–4076

7. Nakanishi, N., Takeuchi, F., and Tsubaki, M. (2007) Histidine cycle mechanism for the concerted proton/electron transfer from ascorbate to the cytosolic heme *b* center of cytochrome b_{561}: a unique machinery for the biological transmembrane electron transfer. *J. Biochem.* **142**, 553–560
8. Rahman, M. M., Nakanishi, N., Takigami, T., Hase, T., Park, S.-Y., and Tsubaki, M. (2007) Purification and biochemical analysis of *Zea mays* cytochrome b561 heterologously expressed in *Pichia pastoris*. In *2007 International Symposium on Micro-Nanomechatronics and Human Science, MHS2007*, pp. 108–112
9. Rahman, M. M., Nakanishi, N., Fujito, M., Miura, M., Hase, T., Park, S.-Y., Hori, H., and Tsubaki, M. (2008) Inhibition of the electron transfer of plant cytochrome b561 by the modification with diethylpyrocarbonate: in search of a common mechanism for the transmembrane electron transfer from ascorbate. In *MHS2008. International Synmposium on Micro-NanoMechatoronics and Human Science, 2008*, pp. 157–162, IEEE, Nagoya
10. Takeuchi, F., Hori, H., and Tsubaki, M. (2005) Selective perturbation of the intravesicular heme center of cytochrome b561 by cysteinyl modification with 4,4′-dithiodipyridine. *J. Biochem.* **138**, 751–762
11. Dutton, P. L. (1978) Redox potentiometry: determination of midpoint potentials of oxidation-reduction components of biological electron-transfer systems. *Methods in Enzymol.* **54**, 411–435
12. Nakanishi, N., Takeuchi, F., Okamoto, H., Tamura, A., Hori, H., and Tsubaki, M. (2006) Characterization of heme-coordinating histidyl residues of cytochrome b_5 based on the reactivity with diethylpyrocarbonate: a mechanism for the opening of axial imidazole rings. *J. Biochem.* **140**, 561–571
13. Nakanishi, N., Takeuchi, F., Park, S.-Y., Hori, H., Kiyota, K., Uno, T., and Tsubaki, M. (2008) Characterization of heme-coordinating histidyl residues of an engineered six-coordinated myoglobin mutant based on the reactivity with diethylpyrocarbonate, mass spectrometry, and EPR spectroscopy. *J. Biosci. Bioeng.* **105**, 604–613
14. Preger, V., Scagliarini, S., Pupillo, P., and Trost, P. (2005) Identification of an ascorbate-dependent cytochrome *b* of the tonoplast membrane sharing biochemical features with members of the cytochrome *b*561 family. *Planta* **220**, 365–375
15. Njus, D. and Kelley, P. M. (1993) The secretory-vesicle ascorbate-regenerating system: a chain of concerted H^+/e^--transfer reactions. *Biochim. Biophys. Acta* **1144**, 235–248
16. Kipp, B. H., Faraj, C., Li, G., and Njus, D. (2004) Imidazole facilitates electron transfer from organic reductants. *Bioelectrochemistry* **64**, 7–13
17. Takigami, T., Takeuchi, F., Nakagawa, M., Hase, T., and Tsubaki, M. (2003) Stopped-flow analyses on the reaction of ascorbate with cytochrome b561 purified from bovine chromaffin vesicle membanes. *Biochemistry* **42**, 8110–8118
18. Bashtovyy, D., Bérczi, A., Asard, H., and Páli, T. (2003) Structure prediction for the di-heme cytochrome b_{561} protein family. *Protoplasma* **221**, 31–40
19. Mayer, J. M. (2004) Proton-coupled electron transfer: a reaction chemist's view. *Ann. Rev. Phys. Chem.* **55**, 363–390
20. Waaren, J. J. and Mayer, J. M. (2008) Hydrogen atom transfer reactions of iron-porphyrin-imidazole complexes as models for histidine-ligated heme reactivity. *J. Am. Chem. Soc.* **130**, 2774–2776